XIX IMEKO World Congress
Fundamental and Applied Metrology
September 6–11, 2009, Lisbon, Portugal

SINGLE-PHASE POWER QUALITY ANALYZER BASED ON A NEW DETECTION AND CLASSIFICATION ALGORITHM

Tomáš Radil [1], *Pedro M. Ramos* [1,2], *A. Cruz Serra* [1,2]

[1] Instituto de Telecomunicações, Lisbon, Portugal
[2] DEEC, Instituto Superior Técnico, Technical University of Lisbon, Lisbon, Portugal
e-mail: tomas.radil@lx.it.pt, pedro.ramos@lx.it.pt, acserra@ist.utl.pt

Abstract – This paper describes a simple power quality analyzer based on a digital signal processor. In this analyzer, a new algorithm for detection and classification of power quality events is implemented. The analyzer detects and classifies in real-time transients, waveform distortions, sags, interruptions and swells.

Keywords: power quality, digital signal processor.

1. INTRODUCTION

In the recent years, the monitoring of power quality (PQ) has become a very important issue. As the number of locations within the power system, where PQ monitoring is required, increases, so does the demand for simple, low-cost and yet reliable PQ analyzers. The performance of the new PQ monitoring algorithms that have been published is usually shown only on simulated signals or on small sets of measured data and also their suitability for implementation in a stand-alone PQ analyzer that could be used for field measurements is rarely discussed.

In this paper, a prototype of a developed power quality analyzer is described. The goal of the development of this analyzer was to design a simple instrument that would allow implementation of custom algorithms for real-time detection and classification of PQ events in the power system. The algorithms can be then tested in field measurements. The PQ analyzer is based on a digital signal processor (DSP) which provides the computational power to perform complex signal processing and is easily reprogrammable. In this PQ analyzer, new algorithms for detection and classification [1] of the most important disturbances that occur in a single-phase power system were implemented.

Section 2 of this paper describes the circuitry of the developed PQ analyzer. Section 3 describes the implemented algorithms for detection and classification of events. Section 4 deals with the implementation and performance of individual employed algorithms.

2. PQ ANALYZER PROTOTYPE

The PQ analyzer (Fig. 1) uses two closed-loop Hall effect transducers to measure the voltage and current in the single-phase 230 V/50 Hz power system. The voltage transducer (V) LEM CV 3-500 has an input range ±500 V and bandwidth 300 kHz. The current transducer (I) LEM LA 25-NP has an input range ±8.5 A and bandwidth 150 kHz. The output signal of the transducers is processed in signal conditioning circuits and digitized using two successive approximation analog-to-digital converters (ADCs). The sampling rate of the ADCs is 50 kS/s and their resolution is 16 bits. The sampling clock of the ADCs is generated by the digital signal processor (DSP) ADSP-21369. The DSP uses its internal precision clock

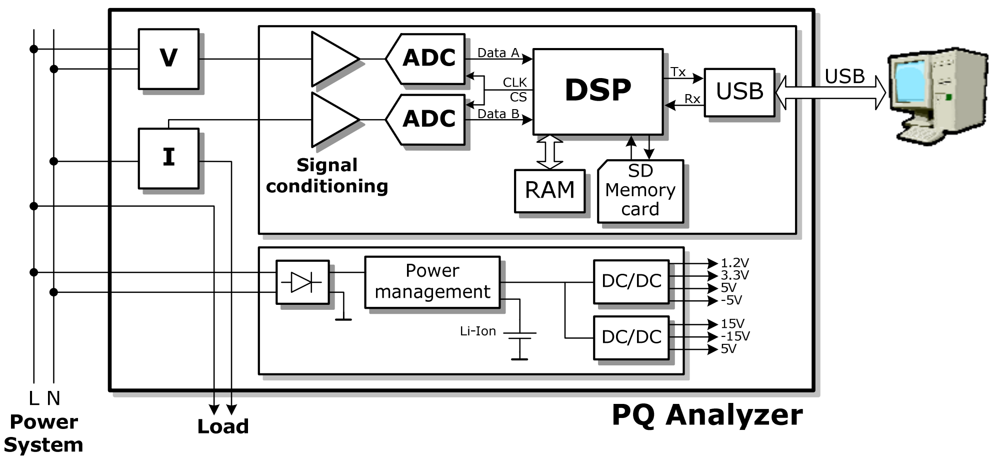

Fig. 1 Block diagram of the proposed PQ analyzer.

generator to produce a stable and low-jitter sampling clock. The ADCs are connected to one of the DSP's two channel synchronous serial ports (SPORT).

Besides controlling the data acquisition process, the DSP also performs all the processing required by the proposed detection and classification algorithm. The selected DSP is a 32-bit floating-point processor running at 262 MHz. The DSP has 2Mbit (64k words) of on-chip memory. Since this memory is not sufficient to store all data and to perform all required processing, a 128Mbit (4M words) synchronous dynamic RAM (SDRAM) is connected to the DSP. The SDRAM memory is used to store auxiliary data and variables required during the processing and to store the acquired data while it is processed and before it is stored on the memory card in case of event detection. The analyzer uses a SD memory card with capacity 1GB to store the waveforms that include the detected events. The SD card is operated using one of the DSP's SPI ports.

When the PQ analyzer is connected to a PC, the detected disturbances can be uploaded via full-speed USB 2.0 interface. The USB functionality is provided by the FT232 chip, which is connected to the DSP's asynchronous serial port.

The PQ analyzer must be able to work even when the voltage in the power network is outside its nominal range. Since the analyzer is powered from the monitored power system, it contains a backup rechargeable Li-Ion battery which is used to power the analyzer during *e.g.* sags and interruptions. The battery is recharged when needed and the voltage in the power system is at its nominal level. The power supply provides battery backed-up power for all the analyzer's electronics and for the voltage and current transducers.

3. OPERATION OF THE PQ ANALYZER

Each measurement cycle starts by acquiring new samples of the digitized voltage and current waveforms. The power quality analyzer processes the waveforms in frames that are 150 000 samples long (this equals to 3 s at sampling rate 50 kS/s). The acquisition of the new samples using the DSP's SPORT is interrupt driven. Since the DSP's internal memory is not sufficient to store 150 000 samples of voltage and current waveforms, first, the acquired samples are stored in small buffers placed in the internal memory and when the buffers are full (the capacity of the buffers is 500 words), their content is transferred to the SDRAM using direct memory access (DMA) to achieve optimal performance and to efficiently use the SDRAM's speed. When all 150 000 samples are acquired and stored in the SDRAM, the PQ analyzer proceeds to the signal processing stage. While processing the recently acquired waveforms, the analyzer continues with the acquisition of the next cycle to ensure continuous monitoring of the power system.

In the signal processing stage, the acquired frame of the voltage waveform is processed. The processing (see Fig. 2) starts by normalizing the voltage waveform; *i.e.*, dividing the voltage samples by the ratio of the nominal RMS value V_{NOM} and voltage sensor coefficient. In this step, eventual corrections (such as corrections of the transducer's nonlinearity) can be introduced.

After pre-processing, the analyzer proceeds to the event detection step. In this step, the processing splits and two different sets of algorithms are applied to the voltage signal in order to detect different power quality disturbances. The first set is used to detect disturbances such as transients and waveform distortions, while the second set is used to detect sags, swells, interruptions, undervoltages and overvoltages.

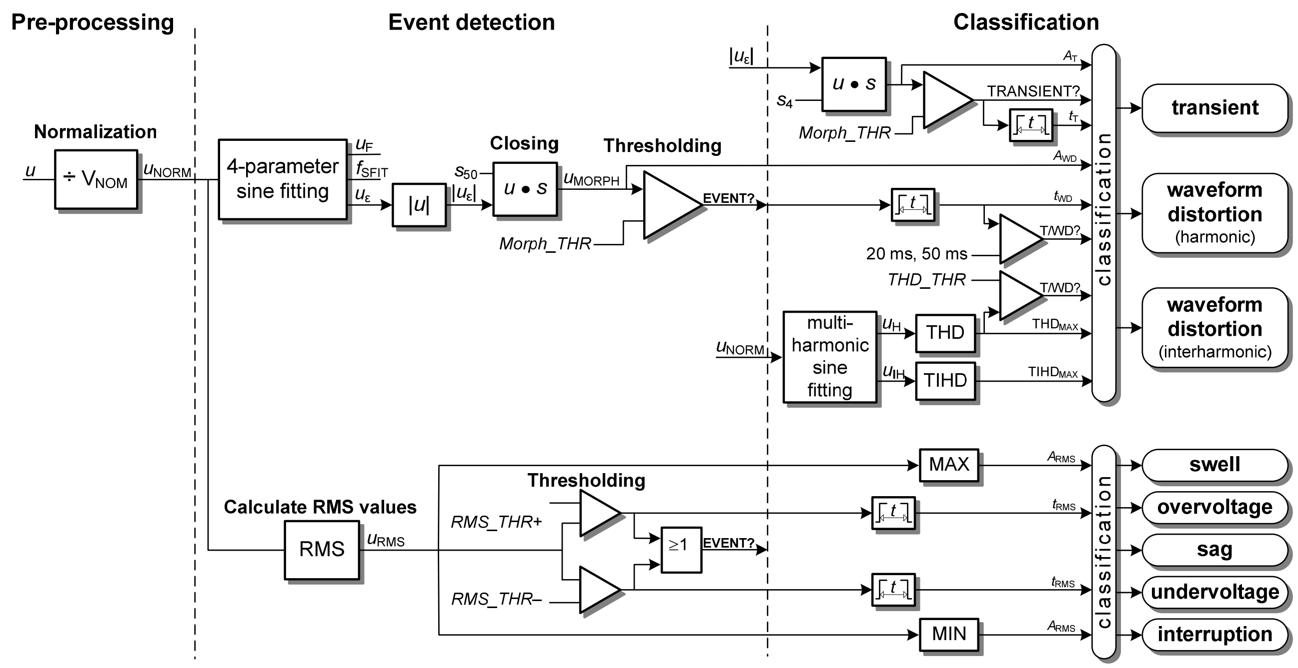

Fig. 2 Block diagram of the detection and classification algorithm implemented in the PQ analyzer.

3.1. Detection and classification of transients and waveform distortions

In order to detect transients and waveform distortions, the fundamental u_F and the non-fundamental u_ε components of the voltage signal u_{NORM} have to be separated

$$u_{\mathrm{NORM}} = u_{\mathrm{F}} + u_{\varepsilon} \ . \tag{1}$$

The 4-parameter sine fitting algorithm [2] is used to separate these components. The initial estimates of the signal's parameters are obtained using the IpDFT algorithm [3] and the 3-parameters sine fitting algorithm [2].

The non-fundamental component u_ε contains the potential disturbances. To simplify the detection process, the absolute value of u_ε is calculated and the resulting signal is processed using the mathematical morphology operation called closing [4][5]

$$u_{\mathrm{MORPH}} = |u_{\varepsilon}| \bullet s_{50} \tag{2}$$

where s_{50} is the so-called structuring element – in this case a signal containing ones whose length is equal to 50 ms (2.5 periods of the nominal fundamental frequency).

The resulting signal u_{MORPH} represents an envelope of the signal $|u_\varepsilon|$. Calculating the envelope simplifies the detection of potential events using thresholding because it removes multiple crossings of the threshold level that belong to a single event. An event is detected when the signal u_{MORPH} crosses the threshold level *Morph_THR*.

In the classification step, the detected events are classified based on their parameters such as duration and the content of harmonic and interharmonic frequencies. The flow chart of the decision process in which the analyzer decides whether the event is a transient or a waveform distortion is shown in Fig. 3. If the duration of the event (t_{WD}) is longer than 50 ms or the duration is longer than 20 ms and, at the same time, the maximum total harmonic distortion (THD) during the event have exceeded the THD_THR threshold level, the event is classified as a waveform distortion (WD). Otherwise, it is classified as a transient (T).

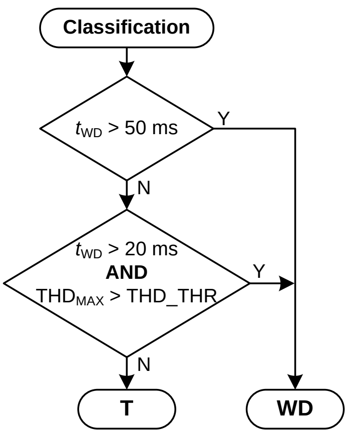

Fig. 3 Flow chart of the classification process – transients and waveform distortions.

The analyzer further distinguishes two types of waveform distortions: harmonic WD and interharmonic WD. The decision is based on the comparison of the maximum THD and the maximum TIHD (total interharmonic distortion) values during the event.

In order to calculate the THD and TIHD value, the analyzer uses the non-iterative multiharmonic sine fitting algorithm [6] to estimate the amplitudes of individual harmonics (up to the 30th). The algorithm uses the final estimate of the frequency f_{SFIT} produced by the 4-parameter algorithm. The multiharmonic sine fitting enables to separate the harmonic u_H and interharmonic u_{IH} parts of the non-fundamental component u_ε

$$u_{\varepsilon} = u_{\mathrm{H}} + u_{\mathrm{IH}} \ , \tag{3}$$

$$u_{\mathrm{H}} = \sum_{h=2}^{30} A_h \cos(h\omega t) + B_h \sin(h\omega t) \ , \tag{4}$$

$$u_{\mathrm{IH}} = u - u_{\mathrm{DC}} - \sum_{h=1}^{30} A_h \cos(h\omega t) + B_h \sin(h\omega t) \tag{5}$$

where A_h and B_h are the parameters of the *h*-th harmonics of the signal u_{NORM}. The part of the signal u_{NORM} that contains the disturbances is divided into one period long frames ($N = 1\,000$ samples) and the multiharmonic sine-fitting is applied to each of these frames. Using the estimated parameters and using the u_{IH} signal, the THD and TIHD values in each frame are calculated

$$\mathrm{THD} = \frac{\sqrt{\sum_{h=2}^{30}\left(A_h^2 + B_h^2\right)}}{\sqrt{A_1^2 + B_1^2}} \ , \tag{6}$$

$$\mathrm{TIHD} = \sqrt{\frac{1}{N}\sum_{n=1}^{N} u_{\mathrm{IH}}^2[n]} \ . \tag{7}$$

The magnitude A_{WD} of a waveform distortion is calculated as the maximum value of the signal u_{MORPH} during the event.

When a transient is detected, the analyzer processes, once again, the signal $|u_\varepsilon|$ using the morphology operation closing. This time, a structuring element s_4 which is 4 ms long is employed. Shorter structuring element enables to separate potential transients that are close to each other in the signal u_{MORPH}. The resulting signal is used to calculate the duration t_T and the magnitude of individual transients A_T.

Detailed description of the algorithm used for detection and classification of transients and waveform distortions can be found in [1].

3.2. Detection and classification of sag, swells and interruptions

While the detection and classification of transients and waveform distortions is based on new algorithms, the detection of sags, swells, interruptions, undervoltages and overvoltages follows the IEC 61000-4-30 standard [7].

The detection uses the calculation of the RMS value of the normalized voltage signal u_{NORM}. The RMS value is calculated every half-period using one period of data

$$u_{\mathrm{RMS}}(j)=\sqrt{\frac{1}{N}\sum_{i=(j-1)N/2}^{(j+1)N/2-1}u_{\mathrm{NORM}}^{2}(i)} \tag{8}$$

where N is the number of samples per period (1 000), j = 1, 2,… 299 (the processed frame is 150 000 samples long).

The detection of events is done by thresholding the u_{RMS} signal with two threshold levels: *RMS_THR–* and *RMS_THR+*. An event is detected when u_{RMS} exceeds *RMS_THR+* or drops below *RMS_THR–*.

The classification of detected events is based on their duration t_{RMS} and magnitude A_{RMS}. For sags, undervoltages and interruptions, A_{RMS} is calculated as the minimum of the u_{RMS} during the event. In case of swells and overvoltages, A_{RMS} is calculated as the maximum value of u_{RMS} during the event. The flow chart of the classification process is shown in Fig. 4.

Events with magnitude below 0.1 pu are classified as interruptions. If the event's magnitude is above 0.1 pu and below the *RMS_THR–* threshold, the event is classified as either sag or undervoltage (depending on its duration). Otherwise (*i.e.* when the event's magnitude is above the *RMS_THR+* level), the event is classified as either swell or overvoltage.

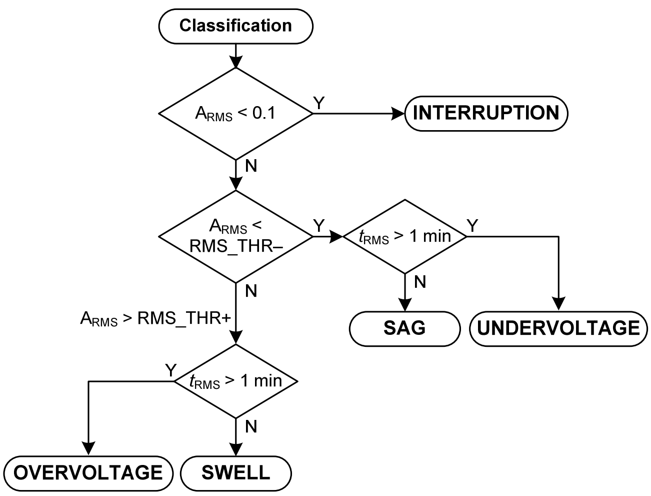

Fig. 4 Flow chart of the classification process – sags, undervoltages, interruptions, swells and overvoltages.

4. IMPLEMENTATION OF THE ALGORITHMS

Implementation of any algorithm into a DSP has to deal with limited resources that the processor offers, especially when the algorithms must work in real-time as in the case of PQ analyzers. In order to achieve maximum performance, the implementation of every algorithm has to respect the limitations of the particular processor. For example: the DSPs usually contain a fast but very small internal memory. Therefore, large data and variables have to be stored in external memory, which is several times slower than the internal memory. An efficient implementation has to maximize the use of direct memory access (DMA) and in case of SDRAM also of block transfers in order to efficiently use the external memory.

4-parameter sine fitting

The 4-parameter sine fitting algorithm, which is used to extract the potential disturbances such as transients and waveform distortions, processes data frames that are N = 150 000 samples long. According to the standard [2] this would mean building a matrix with dimension 150 000×4 (see (46) in [2]). Such a matrix would not fit into the DSP's internal memory and would have to be stored in external memory which would significantly reduce the calculation speed. The following optimization was implemented in order to decrease both the memory requirements and the required computational time.

The algorithm estimates the parameters of the fundamental (in-phase A and quadrature B component, frequency f_{SFIT}, dc component C) by solving the following equation [2]

$$\begin{bmatrix} A & B & C & f_{\mathrm{SFIT}} \end{bmatrix}^{T}=\left(\mathbf{D}^{T}\mathbf{D}\right)^{-1}\left(\mathbf{D}^{T}u_{\mathrm{NORM}}\right) \tag{9}$$

where

$$\mathbf{D}=\begin{bmatrix}\cos(\omega\boldsymbol{t}) & \sin(\omega\boldsymbol{t}) & 1 & -A\boldsymbol{t}\sin(\omega\boldsymbol{t})+B\boldsymbol{t}\cos(\omega\boldsymbol{t})\end{bmatrix} \tag{10}$$

and $\boldsymbol{t}$ is the vector of time stamps.

The algorithm can be optimized by direct calculation of the matrices ($\mathbf{D}^{\mathrm{T}}\mathbf{D}$) and ($\mathbf{D}^{\mathrm{T}}u_{\mathrm{NORM}}$). The matrix ($\mathbf{D}^{\mathrm{T}}\mathbf{D}$) is calculated as

$$\left(\mathbf{D}^{T}\mathbf{D}\right)=\begin{bmatrix} E_{1,1} & E_{1,2} & E_{1,3} & E_{1,4} \\ E_{1,2} & E_{2,2} & E_{2,3} & E_{2,4} \\ E_{1,3} & E_{2,3} & E_{3,3} & E_{3,4} \\ E_{1,4} & E_{2,4} & E_{3,4} & E_{4,4} \end{bmatrix} \tag{11}$$

where

$$E_{1,1}=\sum_{i=1}^{N}\cos^{2}(\omega t_i);\; E_{1,2}=\sum_{i=1}^{N}\sin(\omega t_i)\cos(\omega t_i)\;;$$

$$E_{1,3}=\sum_{i=1}^{N}\cos(\omega t_i)\;;$$

$$E_{1,4}=\sum_{i=1}^{N}\cos(\omega t_i)\left[-At_i\sin(\omega t_i)+Bt_i\cos(\omega t_i)\right]\;;$$

$$E_{2,2}=\sum_{i=1}^{N}\sin^{2}(\omega t_i)\; E_{2,3}=\sum_{i=1}^{N}\sin(\omega t_i)\;;$$

$$E_{2,4}=\sum_{i=1}^{N}\sin(\omega t_i)\left[-At_i\sin(\omega t_i)+Bt_i\cos(\omega t_i)\right]\;;$$

$$E_{3,3}=N;\quad E_{3,4}=\sum_{i=1}^{N}\left[-At_i\sin(\omega t_i)+Bt_i\cos(\omega t_i)\right]\;;$$

$$E_{4,4}=\sum_{i=1}^{N}\left[-At_i\sin(\omega t_i)+Bt_i\cos(\omega t_i)\right]^{2}.$$

Note that ($\mathbf{D}^{\mathrm{T}}\mathbf{D}$) is a symmetric matrix and the element $E_{3,3}$ is constant (equal to the number of samples N). Therefore, only 9 out of 16 elements have to be calculated.

The matrix ($\mathbf{D}^{\mathrm{T}}u_{\mathrm{NORM}}$) is

$$\left(\mathbf{D}^T u_{\text{NORM}}\right) = \begin{bmatrix} \sum_{i=1}^{N} u_{\text{NORM}}[i]\cos(\omega t_i) \\ \sum_{i=1}^{N} u_{\text{NORM}}[i]\sin(\omega t_i) \\ \sum_{i=1}^{N} u_{\text{NORM}}[i] \\ \sum_{i=1}^{N} u_{\text{NORM}}[i]\left[-At_i\sin(\omega t_i) + Bt_i\cos(\omega t_i)\right] \end{bmatrix}. \quad (12)$$

The matrices ($\mathbf{D}^T\mathbf{D}$) and ($\mathbf{D}^T u_{\text{NORM}}$) have dimension 4×4 and 4×1, respectively, whereas the matrix **D** had dimension N×4. From this it can be seen that the direct calculation of the matrices ($\mathbf{D}^T\mathbf{D}$) and ($\mathbf{D}^T u_{\text{NORM}}$) requires significantly less amount of memory. It is also more computationally efficient because it avoids the matrix operations with the big matrix **D**. Both matrices ($\mathbf{D}^T\mathbf{D}$) and ($\mathbf{D}^T u_{\text{NORM}}$) can be stored in DSP's fast internal memory.

Similar modifications can be also applied to the 3-parameter sine fitting algorithm, which is used for the initial estimation of the parameters of the voltage signal's fundamental.

In this application, the direct calculation of the matrices ($\mathbf{D}^T\mathbf{D}$) and ($\mathbf{D}^T u_{\text{NORM}}$) decreased the required computational time by 30% (approximately 200 ms). For more information on the computational requirements see the sub-section "Overall performance".

Closing operation

The proposed detection and classification algorithm uses the closing operation to obtain the envelope of the signal containing potential disturbances. The closing operation is defined using two other mathematical morphology operations [4]: dilation ⊕ and erosion ⊖

$$u_{\text{MORPH}} = |u_\varepsilon| \bullet s_{50} = \left(|u_\varepsilon| \oplus s_{50}\right) \ominus s_{50}\,. \quad (13)$$

The output of the dilation operation is calculated by shifting the structuring element s_{50} (which is long N_S = 2 500 samples) along the processed signal $|u_\varepsilon|$ (N = 150 000) and calculating the maximum value of the samples that belong to the neighbourhood defined by the current position of the structuring element. The erosion operation is similar, only this time the minimum value is calculated.

Implementation of the closing operation according to this definition would be very inefficient. Both the dilation and the erosion operation would require N_S accesses to each sample of the processed signal. Due to the length of $|u_\varepsilon|$, the signal has to be stored in the external (relatively slow) SDRAM memory making the calculation of the closing operation even slower.

In the described PQ analyzer, the dilation and erosion operations are implemented using the Herk-Gil-Werman algorithm [8][9]. The Herk-Gil-Werman implementation of dilation and erosion requires only $3 - 4/N_S$ accesses to each sample each thus significantly reducing the number of accesses to the external memory. For large N_S, the Herk-Gil-Werman algorithm does not depend on the length of the structuring element, which can be seen from Table 1. From this table it follows that the closing operation using the structuring element s_{50} (N_S = 2 500 samples) takes almost the same time as the closing operation using s_4 (N_S = 200 samples).

Overall performance

Table 1 shows an example of computational times required by individual algorithms employed in the detection and classification process. The processing times in this example were achieved while processing one frame (150 000 samples) of measured data.

The acquisition of the 3 s frame of data takes only 19.81 ms of processor time leaving enough time to process the previous frame.

The signal used to test the part detecting transients and waveform distortions contained 2 transients. The second part was tested using a signal containing one sag. The iterative part of the 4-parameter sine fitting algorithm converged after two iterations (*i.e.*, 233.93 ms were required to perform 2 iterations of the algorithm).

The individual algorithms were tested separately; *i.e.* when measuring the time required to detect and classify the disturbances the data acquisition was stopped and vice versa. Therefore, the total time required by all the algorithms is slightly bigger (by few tens of milliseconds) than the mere sum of times in Table 1. This is caused by *e.g.* the conflicts between the DMA transfer that writes the acquired data to the SDRAM and the DMA transfer (and also normal accesses) used to obtain data from the SDRAM for processing.

The PQ analyzer is able to work in real-time because the total time required by individual algorithms is significantly lower than the duration of one frame (3 s).

Table 1. Processing times required by individual algorithms.

Algorithm	Time
Data acquisition Reading samples from the ADCs, configuring DMA transfer to the SDRAM	19.81 ms
Transients and waveform distortions IpDFT and 3-parameter sine fitting	115.67 ms
4-parameter sine fitting (initial part)	116.96 ms
4-parameter sine fitting (iterative part)	233.93 ms
Calculation of abs. value and u_ε signal	108.67 ms
Closing operation (s_{50})	34.21 ms
Event detection	20.82 ms
Closing operation (s_4)	33.66 ms
Classification	267.89 ms
Sags, interruptions, swells,… RMS calculation	20.75 ms
Event detection	16.47 µs
Classification	12.87 µs

5. CONCLUSIONS

The described PQ analyzer represents a simple and flexible instrument that allows testing of custom designed detection and classification algorithms in field measurements and monitoring. The analyzer implements a new algorithm for detection and classification of transients and waveform distortions that is based on sine fitting algorithms and a conventional algorithm for detection of sags, swells and interruptions.

ACKNOWLEDGMENTS

Work sponsored by the Fundação para Ciência e Tecnologia.

REFERENCES

[1] T. Radil, P. M. Ramos, A. C. Serra, "Improved Method for Detection and Classification of Transients and Waveform Distortions Using Sine Fitting Algorithms", *ICREPQ'09*, Valencia, Spain, 2009.

[2] *IEEE Std 1057-1994, IEEE Standard for Digitizing Waveform Recorders*, The Institute of Electrical and Electronics Engineers, Inc., New York, 1995.

[3] H. Renders, J. Schoukens, G. Vilain, "High-Accuracy Spectrum Analysis of Sampled Discrete Frequency Signals by Analytical Leakage Compensation", *IEEE Trans. Instr. Meas.*, vol. 33, no. 4, pp. 287 – 292, Dec. 1984.

[4] J. Serra. *Image Analysis and Mathematical Morphology*, volume 1. Academic Press, 1982

[5] T. Radil, P. M. Ramos, F. M. Janeiro, A. C. Serra, "DSP Based Power Quality Analyzer for Detection and Classification of Disturbances in a Single-phase Power System", *Metrology and Measurement Systems*, Vol. XIV, No. 4, pp. 483 - 494, December, 2007.

[6] P. M. Ramos, M. F. da Silva, R. C. Martins, A. M. C. Serra, "Simulation and experimental results of multiharmonic least-squares fitting algorithms applied to periodic signals," *IEEE Trans. Instrum. Meas.*, vol. 55, no. 2, pp. 646-651, Apr. 2006.

[7] IEC 61000-4-30 Electromagnetic compatibility (EMC) - Part 4-30: Testing and measurement techniques (Power quality measurement methods), 2003.

[8] M. van Herk, "A fast algorithm for local minimum and maximum filters on rectangular and octagonal kernels," *Pattern Recognition Letters* 13, pp. 517–521, July 1992

[9] J. Y. Gil, M. Werman, "Computing 2-D min, median and max filters," *IEEE Trans. Pattern Analysis and Machine Intelligence*, vol. 15, no. 5, pp. 504–507, May 1993